



RESEARCH ARTICLE | NOVEMBER 08 2022

Toward defect-free components in laser metal deposition with coaxial wire feeding through closed-loop control of the melt pool temperature ^{EP}

Special Collection: [Laser Additive Manufacturing Processes: From Cladding to Complex Parts](#)

Christian Bernauer  ; Avelino Zapata  ; Michael F. Zaeh



J. Laser Appl. 34, 042044 (2022)

<https://doi.org/10.2351/7.0000773>



Articles You May Be Interested In

Real-time monitoring and control of the layer height in laser metal deposition with coaxial wire feeding using optical coherence tomography

J. Laser Appl. (October 2024)

Effect of heat accumulation on the single track formation during laser metal deposition and development of a framework for analyzing new process strategies

J. Laser Appl. (December 2020)

New method for high-efficiency keyhole-based wire direct energy deposition: Process innovation and characterization

J. Laser Appl. (July 2024)

11 March 2025 13:03:48





Toward defect-free components in laser metal deposition with coaxial wire feeding through closed-loop control of the melt pool temperature



Cite as: J. Laser Appl. 34, 042044 (2022); doi: 10.2351/7.0000773
Submitted: 23 June 2022 · Accepted: 27 September 2022 ·
Published Online: 8 November 2022



Christian Bernauer,  Avelino Zapata,  and Michael F. Zaeh

AFFILIATIONS

Technical University of Munich, TUM School of Engineering and Design, Institute for Machine Tools and Industrial Management (iwb), Boltzmannstrasse 15, 85748 Garching, Germany

Note: Paper published as part of the special topic on Laser Additive Manufacturing Processes: From Cladding to Complex Parts.

ABSTRACT

Laser metal deposition (LMD) is an additive manufacturing process in which a metal powder or wire is added to a laser-induced molten pool. This localized deposition of material is used for the manufacturing, modification, and repair of a wide range of metal components. The use of wire as feedstock offers various advantages over the use of powder in terms of the contamination of the process environment, the material utilization rate, the ease of handling, and the material price. However, to achieve a stable process as well as defined geometrical and microstructural properties over many layers, precise knowledge on the effects of the input variables of the process on the resulting deposition characteristics is required. In this work, the melt pool temperature was used as an input parameter in LMD with coaxial wire feeding of stainless steel, which was made possible through the use of a dedicated closed-loop control system based on pyrometry. Initially, a temperature range was determined for different process conditions in which a stable deposition was obtained. Within this range, the cause-effect relationships between the melt pool temperature and the resulting geometry as well as the material properties were investigated for individual weld beads. It was found that the melt pool temperature is positively correlated with the width of the weld bead as well as the dilution. In addition, a dependence of the microhardness distribution over the cross section of a weld bead on the melt pool temperature was demonstrated, with an increased temperature negatively affecting the hardness.

Key words: laser metal deposition, coaxial wire feeding, additive manufacturing, closed-loop temperature control, annular laser beam, directed energy deposition, melt pool temperature

© 2022 Author(s). All article content, except where otherwise noted, is licensed under a Creative Commons Attribution (CC BY) license (<http://creativecommons.org/licenses/by/4.0/>). <https://doi.org/10.2351/7.0000773>

I. INTRODUCTION

Additive manufacturing (AM) of metal components is steadily gaining importance in various industries such as aerospace, mold tooling, automotive, and oil and gas.¹ For this increased industrial relevance, laser technologies are key enablers, as they allow for localized melting of material due to the highly focused and controlled energy input. Laser metal deposition (LMD) is one of the most economically relevant laser-based AM processes. In LMD, a filler material in the form of powder or wire is fed into a laser-induced melt pool. After solidification, a new material layer remains on the part. This can be used for the deposition of

functional coatings, for the repair of high-value parts, and for the manufacturing of complex three-dimensional components.² In contrast to the widely used AM processes employing a powder bed, LMD exhibits significantly higher deposition rates and enables the deposition on existing free-form surfaces. In addition, compared to arc welding processes, the defined energy input results in a relatively small heat-affected zone and low residual stresses. Wire as feedstock material is increasingly demanded by the industry since it is readily available, inexpensive, easy to handle, and results in less contamination of the process environment than powder.³ To overcome the directional dependence of lateral wire feeding, which is state of the art, recent developments in beam shaping optics allow

11 March 2025 13:03:48

for coaxial feeding of the wire inside a hollow laser beam⁴ or in the center of several single laser beams.⁵

A major challenge in LMD arises from the layered buildup, as defects are often amplified over many layers. Furthermore, changing thermal boundary conditions in higher layers or in small features can lead to heat accumulation, which results in an unstable process as well as highly inhomogeneous or defective components.⁶ To ensure consistent and stable process conditions without extensive parameter studies, approaches for monitoring and closed-loop control are essential. This particularly applies to wire-based LMD since self-regulating effects due to overspray do not occur as in the powder-based process variant.⁷ One of the most critical variables regarding the process stability and the quality of the deposition is the melt pool temperature. Using pyrometers or infrared (IR) cameras, the melt pool temperature can be measured online and, thus, be adjusted by means of a closed-loop control. For this, the laser power is commonly used as the manipulated variable.⁸ One advantage of using a pyrometer for the temperature measurement is the immediate availability of a real-time temperature signal without computationally intensive image processing steps. A dedicated closed-loop control system based on a well-calibrated pyrometer signal, thus, enables the melt pool temperature to be specified as an input parameter for the process. However, although a controlled temperature can facilitate maintaining constant process conditions, the effects of different reference temperatures need to be well understood.

A number of works investigated the cause-effect relationships between the melt pool temperature and the resulting part properties in an open-loop process. Hua *et al.*⁹ used an off-axis pyrometer in powder-based LMD to evaluate the effect of the main process parameters on the melt pool temperature. It was demonstrated that the powder feed rate, the traverse speed, and the laser spot diameter were negatively correlated with the melt pool temperature, while there was a positive correlation with the laser power. The influence of the shielding gas flow on the temperature could be neglected in the experiments performed. Using a similar experimental setup with an off-axis pyrometer, these observations were confirmed by Bi *et al.*¹⁰ with the laser power showing the strongest influence. In a further study, Bi *et al.*¹¹ revealed that based on the melt pool temperature, conclusions about the process stability can be drawn and that larger temperature deviations lead to dimensional errors as well as an inhomogeneous microstructure and hardness. Pavlov *et al.*¹² as well as Doubenskaia *et al.*¹³ used a setup with a multi-wavelength pyrometer and an IR camera to monitor the process zone temperatures in powder-based LMD. In both works, for the laser power and for the traverse speed, the findings of Refs. 9 and 10 were validated, while it was found that the powder feed rate had no significant influence on the melt pool temperature for the given experimental setup. Furthermore, Doubenskaia *et al.*¹³ reported a nearly linear increase in the bead height and the dilution with increasing melt pool temperatures. For wire-based LMD, Kotar *et al.*¹⁴ used an in-axis pyrometer to demonstrate a positive correlation of the average melt pool temperature with the laser power and a negative correlation with the wire feed rate. These correlations were attributed to the influence of the energy per unit volume on the melt pool temperature. In wire-based LMD, contrary to the melt pool temperature, the main process parameters,

i.e., wire feed rate, traverse speed, and laser power, and their effects on the deposition characteristics were discussed thoroughly in several studies.^{14–17}

In all studies presented, however, the melt pool temperature could not be adjusted in a defined way. Various works addressed the design of thermal control systems in LMD and demonstrated the increased stability of a thermally controlled process.^{18–23} However, only a few studies dealt with the effects of controlled process zone temperatures on the resulting deposition characteristics. Regarding the melt pool temperature in powder-based LMD, Song and Mazumder¹⁹ and Smoqi *et al.*²² observed that maintaining a constant temperature level through a pyrometer-based closed-loop control improved the homogeneity of the microstructure and the microhardness distribution. Furthermore, Salehi and Brandt²⁴ showed that a proportional integral derivative controller can improve the quality of deposited coatings in powder-based LMD. The melt pool temperature was measured using an in-axis pyrometer and the laser power was adjusted by the controller to track the reference temperature. It was demonstrated that particularly low temperatures as well as high feed rates tended to result in an unstable process. However, these correlations were only evaluated for a small range of parameters.

The overall insufficient literature on thermal control of wire-based LMD and the lack of studies on the cause-effect relationships between the melt pool temperature and the deposition characteristics served as motivating factors for the present research work. Consequently, a dedicated closed-loop control system was employed to specify the melt pool temperature in a defined way and, thus, examine the influence on the process stability and the resulting weld bead properties thoroughly. Hence, the melt pool temperature was utilized to substitute the laser power as an input parameter of the process. First, a process window containing the setpoint temperatures that could be tracked in a stable manner was determined. Subsequently, the correlations between the temperature and the weld bead characteristics were evaluated in detail within this process window.

II. MATERIALS AND METHODS

A. Materials

As feedstock material, a standard stainless steel ER316LSi welding wire with a diameter of 1 mm was used. Sandblasted plates of austenitic stainless steel AISI 304 with dimensions of 100 × 100 × 10 mm³ served as substrate material. Before the experiments, the plates were cleaned with isopropanol to remove existing contaminants.

B. Experimental setup

The core of the experimental setup was a wire deposition head (CoaxPrinter, Precitec GmbH & Co. KG, Germany) that enabled coaxial feeding of the wire inside an annular laser beam profile. Consequently, a direction-independent LMD process was possible. The laser beam source used was a 4 kW disk laser (TruDisk 4001, TRUMPF GmbH & Co. KG, Germany) emitting at 1030 nm in continuous wave mode. The laser radiation was guided to the wire deposition head by a fiber optic cable with a core diameter of

11 March 2025 13:03:48

600 μm . In the process zone, a maximum achievable laser power of only 3756 W was experimentally determined, which is due to radiation losses in the optical components. These losses are taken into account for all laser powers given in the following. The feedstock was provided by an industrial wire feeding unit (DIX FDE PN 100 L, DINSE GmbH, Germany). To compensate for the curvature of the wire, which was delivered in a coil, a precisely adjusted two-plane wire straightening unit was used. An accurate positioning of the wire deposition head was enabled by a six-axis industrial robot (KR 60 HA, KUKA AG, Germany) with a maximum payload of 60 kg, which was actuated by a robotic control system (KR C4, KUKA AG, Germany).

For a coaxial measurement of the melt pool temperature T_m , a pyrometer (METIS M322, Sensortherm GmbH, Germany) in one-color mode (sensitive in the range of 1.45–1.65 μm) with a temperature measurement range of 600–2300 $^{\circ}\text{C}$ was mounted to the wire deposition head. Although the pyrometer also featured a two-color mode, it was used in one-color mode due to the significantly lower noise in the signal.²⁵ A precise calibration of the pyrometer to measure the surface temperature of the melt pool was carried out, following the procedure described by Zapata *et al.*²⁵ The focal position of the processing laser beam was set at -6 mm (below the surface of the substrate), resulting in an annular laser spot with an outer diameter of 2.75 mm. According to Ref. 25, a medium-sized pyrometer spot with an outer diameter of 2.4 mm was adjusted through an individual focusing unit to ensure a measurement entirely within the melt pool. For the experiments conducted, a possible temperature dependence of the emissivity was considered negligible.²⁶

The processing of the measurement and control signals and the data acquisition were carried out by a programmable logic controller with a sampling rate of 1 kHz. To control the melt pool temperature, a proportional integral controller was used. The controller design is described in Ref. 27. For the closed-loop system, a bandwidth in the range of a few hertz was obtained. The closed-loop control algorithm was implemented on the internal microcontroller of the pyrometer. The laser power P_L served as the manipulated variable and was set by the controller based on the temperature signal. In Fig. 1, the experimental setup is presented schematically together with the main information streams of the system.

C. Experimental procedure

The purpose of the deposition experiments was a detailed investigation of different melt pool temperatures in LMD with coaxial wire feeding. For this, first, a range of melt pool temperatures that could be adjusted by the control system in a stable and defect-free manner was determined. Therefore, individual weld beads with a length of 85 mm were deposited on the substrate plates, whereby the reference temperature was systematically varied in steps of 40 K. Based on Ref. 16, three parameter sets were selected for the investigations, such that a low, a medium, and a high deposition rate were evaluated. A constant speed ratio v_r between the wire feed rate v_w and the traverse speed v_t of 1 was applied to ensure comparability between the different parameter sets. The parameter sets, which are designated A, B, and C, are given in Table I. The different deposition rates used resulted in a

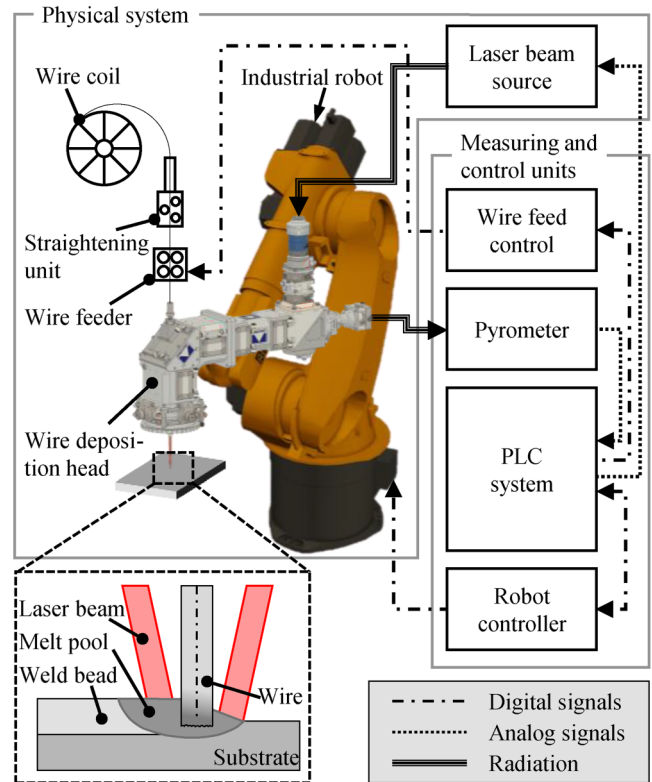


FIG. 1. Configuration of the closed-loop controlled LMD system with coaxial wire feeding.

large range of thermal boundary conditions due to the varying volumes of material to be melted in a given time. During all experiments, the laser power P_L was commanded by the controller. Between the trials, it was ensured that the substrate plate had cooled down to room temperature. In order to reduce oxidation, a constant shielding gas flow (argon) of 20 l/min was applied.

Based on a visual inspection, the weld beads produced were evaluated for the defect patterns of dripping or stubbing, which are typical for wire-based LMD.^{16,28} Furthermore, the logged melt pool temperature signals were analyzed (see Sec. III A) to verify whether the setpoint temperature was reliably attained. An experiment

TABLE I. Process parameters for the temperature controlled deposition of individual weld beads.

Parameter set	A	B	C
Wire feed rate v_w	0.5 m/min	1.0 m/min	1.5 m/min
Traverse speed v_t	0.5 m/min	1.0 m/min	1.5 m/min
Range of laser power P_L	75–3756 W		
Focal position	-6 mm		
Shielding gas flow	20 l/min		

11 March 2025 13:03:48

result was classified as good if no defects occurred during the deposition and the average temperature over the considered track range deviated by no more than 5 K from the reference temperature. These samples labeled as good were subsequently further examined for their resulting weld bead characteristics.

D. Characterization

To determine the cause-effect relationships between the melt pool temperature and the weld bead geometry, the samples were scanned employing a 3D profilometer (VR-3100, Keyence Corporation, Osaka, Japan). Using the software provided by the manufacturer, thermal distortions of the substrate plates were compensated. The width w and the height h of each bead were measured at three positions and the mean value was calculated. In Fig. 2, the relevant dimensions of a weld bead are shown schematically.

For the metallographic analysis and the examination of the degree of dilution, cross sections taken from the beads were polished to $1\ \mu\text{m}$ and subsequently treated with an etching solution (Adler). To evaluate the cross sections, a laser scanning confocal microscope (VK-X 1000, Keyence Corporation, Osaka, Japan) was applied. The degree of dilution η is an important quality criterion when applying functional coatings as well as in additive manufacturing as it allows the mixing of the feedstock with the substrate material or the previous layer to be quantified. It strongly depends on the energy per unit length, the molten mass per unit length, and the heat conduction conditions in the substrate. The degree of dilution was defined as the ratio between the remelted area under the substrate surface A_s and the total melted area ($A_s + A_b$) in the cross section of a bead,¹⁴

$$\eta = \frac{A_s}{A_s + A_b}.$$

Here, A_b is the cross-sectional area of the weld bead (see Fig. 2). For every bead, a mean value from the determined degrees of dilution at three positions was calculated.

On individual cross sections, Vickers microhardness measurements according to DIN EN ISO 6507-1 were subsequently performed employing a fully automated hardness tester (Qness 60 A+ EVO, ATM Qness GmbH, Mammeln, Germany). Based on the literature and preliminary measurements, hardness values between 180 HV and 270 HV were expected. Therefore, the test force was set to 0.9807 N, which corresponds to HV0.1, as suggested by DIN

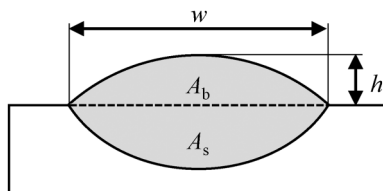


FIG. 2. Characteristics of a weld bead: width w , height h , remelted area A_s , and deposited area A_b .

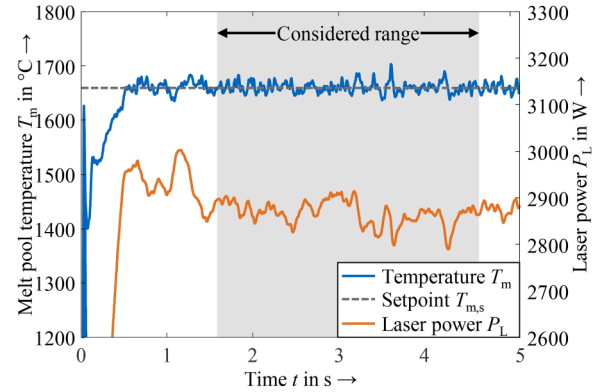


FIG. 3. Melt pool temperature and laser power set by the controller during the deposition of a weld bead using parameter set B and a setpoint temperature of $1660\ \text{°C}$.

EN ISO 6507-4. The dwell time was set to 10 s. For the areal hardness mappings, the distance between the center points of two adjacent indentations was set to $90\ \mu\text{m}$, which corresponded to approximately three times the diagonal length of the indentations. The resulting hardness maps were plotted using MATLAB R2021a.

III. RESULTS AND DISCUSSION

A. Process window

For each of the investigated parameter sets, the reference melt pool temperature to be tracked by the controller was systematically varied to determine the range in which a stable and defect-free process was present. An exemplary temperature curve is shown in Fig. 3 together with the corresponding laser power. At the beginning of the process, it took approximately 500 ms to reach a steady state at the specified temperature. Thereafter, the temperature was maintained at a constant level over the entire track. In order to achieve this, the laser power had to be lowered continuously by the controller due to the increasing substrate temperature resulting from the continuous energy input.

The resulting stable temperature ranges for the three parameter sets investigated are illustrated in Fig. 4. Applying parameter set A, defect-free samples were obtained for temperatures between 1500 and $1700\ \text{°C}$. At $1460\ \text{°C}$, defects occurred in the form of stubbing. At this temperature, which is only slightly above the melting temperature of $1450\ \text{°C}$,²⁹ a stable process could not be maintained due to the low energy input. In contrast, for $1740\ \text{°C}$, the resulting energy input per unit length was too high, leading to droplet formation. For parameter sets B and C, the stable range was significantly larger than for parameter set A. In both cases, stubbing occurred at $1500\ \text{°C}$. Using parameter set B, the highest temperature at which a defect-free deposition could be achieved was $1940\ \text{°C}$. With parameter set C, temperatures above $1980\ \text{°C}$ could not be attained, as the maximum output power of the laser beam source was reached.

The results indicate that, with the given setup, the melt pool can be superheated by 15%–31% above the melting temperature

11 March 2025 13:03:48

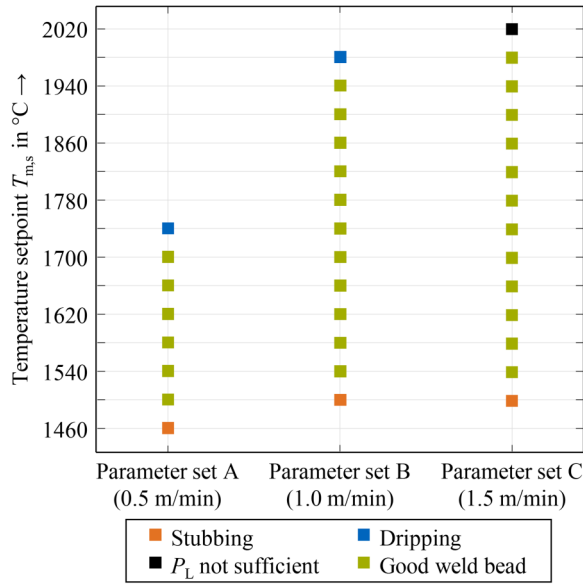


FIG. 4. Stable range of melt pool temperatures for the three parameter sets investigated.

without defects occurring, depending on the parameter set. At higher feed rates, more of the energy supplied was utilized to melt the wire and the substrate, which is why an unstable process and defects occurred at higher temperatures. Regarding this process window, it is noteworthy that in particular at the maximum and minimum setpoint temperatures, the process can become unstable despite the closed-loop process control when thermal boundary conditions change, for example, due to a variation of the substrate thickness. This has to be considered when selecting a setpoint temperature for a specific application case.

For a quantification of the existing fluctuations in the temperature signal, the standard deviations at the respective setpoint temperatures were calculated. In order to consider only the steady-state range of the process, the data obtained within the first 25 mm as well as the last 8 mm of the weld beads were omitted, as indicated in Fig. 3. Due to the different mean temperatures, the coefficient of variance c_v , i.e., the ratio of the standard deviation to the mean value, was determined. This relative measure of variance in the temperature signal is shown in Fig. 5(a) for the experiments carried out.

The fluctuations in the temperature signal tended to increase significantly with higher setpoint temperatures. This can be explained by the increasingly dynamic melt pool at higher temperatures. Since the control system was mainly designed to compensate for changing heat sink capacities and had a bandwidth of a few hertz, these high-frequency fluctuations were not counteracted. For parameter set C, the coefficient of variation decreased at high temperatures. This is due to the fact that the maximum laser power was temporarily reached during the deposition. Because of this saturation, deviations in the temperature signal were compensated more slowly, while the setpoint temperature

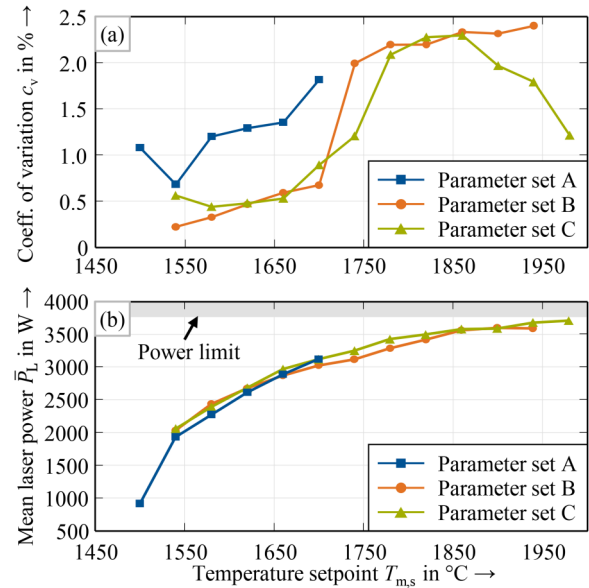


FIG. 5. (a) Coefficients of variation of the melt pool temperature signals; (b) mean laser powers over the steady-state range of the process.

was still reached by the mean value due to the integral term in the controller.

Furthermore, the mean laser powers \bar{P}_L of the respective experiments over the considered range are given in Fig. 5(b). As could be expected, the laser power was consistently increased for higher setpoint temperatures. However, the increase in the required power is nonlinear and tends to stagnate at higher temperatures. In addition, only minor differences are apparent in the required laser powers at different deposition rates. These observations suggest that the conditions of heat transport directly at the melt pool surface change only marginally for the different parameter sets, and the heat dissipation toward the substrate remains virtually constant. In the melt pool, the finite rate of heat conduction inevitably results in a temperature gradient, with the highest temperature occurring at the melt pool surface, i.e., the point of incidence of the laser beam and the origin of the radiation detected by the pyrometer, respectively. In this context, it is also relevant that the thermal conductivity of stainless steel increases for higher temperatures.²⁹ Due to the constant heat dissipation virtually independent of the parameter set used, there are only minor differences in the average laser powers at a given setpoint temperature. Given the different traverse speeds, this results in large differences in the energy per unit length, which is particularly evident for the dilution of the weld beads (see Sec. III C).

B. Influence of the melt pool temperature on the geometric track characteristics

Within the determined stable temperature ranges, the influence of the melt pool temperature on the geometry of the weld beads was evaluated. Figure 6 depicts the bead widths w and

11 March 2025 13:03:48

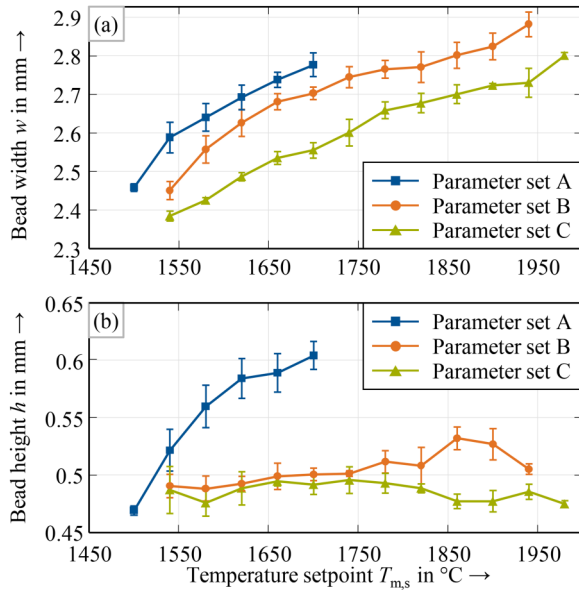


FIG. 6. Influence of the melt pool temperature on (a) the weld bead width w and (b) the weld bead height h .

heights h depending on the setpoint temperature for the three investigated parameter sets. For all parameter sets, a continuous increase in the bead width was observed with increasing temperatures [see Fig. 6(a)]. This confirms previous findings in the literature that there is a positive correlation between melt pool width and melt pool temperature not only for powder-based LMD but also for wire-based LMD.^{23,30} Thus, although in LMD processes the bead width depends primarily on the laser beam diameter on the substrate, an adjustment via the specified melt pool temperature is also possible to a certain extent. The bead width varied between 2.46 and 2.77 mm for parameter set A, 2.45 and 2.88 mm for parameter set B, and 2.38 and 2.80 mm for parameter set C, respectively. This qualitative correlation was also observed for the laser power,^{14–16} which is closely related to the melt pool temperature under constant thermal boundary conditions (see Sec. III A). Since the energy introduced by the laser beam was mainly used to melt either the wire or the substrate material, an increased energy input as a result of a higher laser power led to a larger melt pool. Furthermore, it stands out that significantly larger bead widths were achieved for lower deposition rates at a given temperature. This relationship can be explained by the limited heat conduction rate within the substrate. At a lower traverse speed and a virtually equal energy input [see Fig. 5(b)], a smaller temperature gradient prevailed in the process zone, which allowed for a greater expansion of the melt pool.

Regarding the bead height, only for the parameter set A, a distinct trend with an increasing height for increasing melt pool temperatures is apparent, while for parameter sets B and C no clear correlation with the temperature could be found. The significant increase in the bead height for parameter set A is related to the large melt pool volumes, as discussed in more detail in Sec. III C.

In general, a lower deposition rate results in a greater bead height at a given temperature.

C. Influence of the melt pool temperature on the degree of dilution

The influence of the melt pool temperature on the degree of dilution was evaluated based on cross sections. Figure 7 shows the cross sections of the weld beads with the lowest as well as the highest stable melt pool temperature for each of the three parameter sets investigated. To allow for a direct comparison between the parameter sets at a fixed temperature, the respective samples produced with a setpoint temperature of 1660 °C are displayed.

For all parameter sets, the welding depth was significantly larger at the maximum than at the minimum temperature. This difference was most pronounced for the parameter set A. The effects of the differences in the energy per unit length resulting from the similar average laser powers become clear from the direct comparison at a setpoint temperature of 1660 °C. Despite an identical temperature of the melt pool surface, the melted volume of the substrate was significantly lower with higher feed rates.

Furthermore, Fig. 8 illustrates the degrees of dilution of the good weld beads over the respective setpoint temperatures. As can be observed qualitatively from Fig. 7, the degree of dilution was consistently smaller for higher deposition rates. The minimum values achieved were 37.4% for the parameter set A, 63.7% for the parameter set B, and 52.7% for the parameter set C, while the maximum values were 80.7%, 76.5%, and 71.8%, respectively. Similar to the required mean laser powers (see Fig. 5), asymptotic

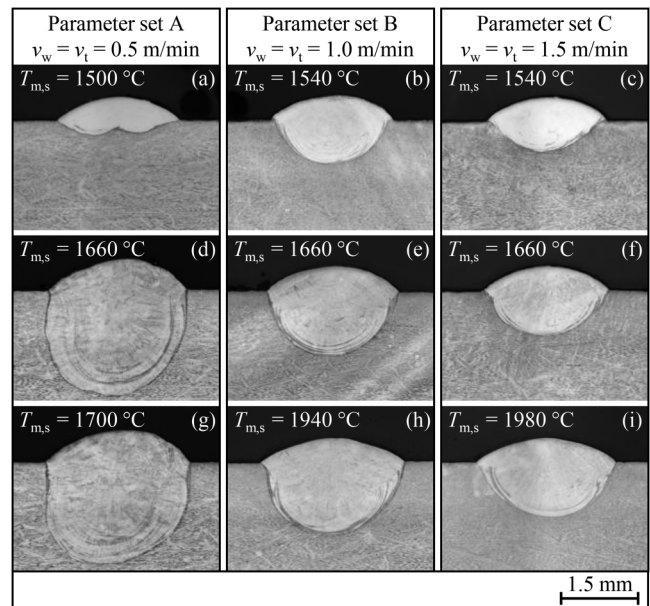


FIG. 7. Cross sections of the weld beads produced with (a)–(c) the minimum stable temperatures, (d)–(f) a temperature of 1660 °C, and (g)–(i) the maximum stable temperatures, respectively.

11 March 2025 13:03:48

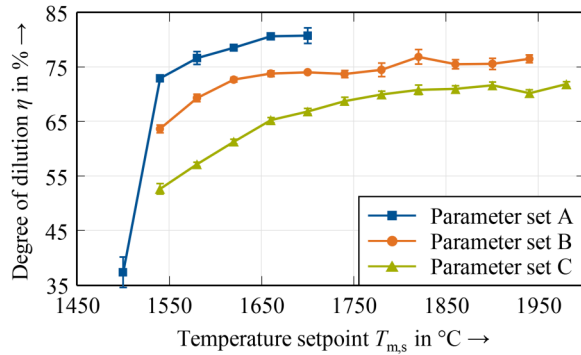


FIG. 8. Influence of the melt pool temperature on the degree of dilution η for the three parameter sets investigated.

curves can be observed, with the degree of dilution varying only slightly with higher temperatures for each parameter set. A lower deposition rate resulted in a significantly larger degree of dilution at a given temperature due to the differences in the energy per unit length described above. With parameter set A, a very low degree of dilution is noticeable at a temperature of 1500 °C. The fact that a stable process was still possible at this temperature in contrast to the other parameter sets is due to the low feed rate and the resulting disproportionately higher energy per unit length. In this experiment, just enough energy was introduced into the melt pool so that the wire was completely melted and no defects occurred, resulting in a low degree of dilution.

Remarkably, an increase in the volume of the deposited weld beads is apparent for higher temperatures in Figs. 6 and 7, respectively, despite the constant speed ratio. This volume change is proportional to the molten pool volume and can possibly be explained by phase transformations³¹ or the formation of intermetallic compounds³² during solidification and cooling. A relation to microporosity is considered improbable since it is practically nonexistent within weld beads produced by wire-based LMD and no pores were detected in any of the cross sections examined. However, an in-depth investigation of the underlying mechanisms is beyond the scope of this work and should be addressed in future studies.

D. Microhardness distribution of selected cross sections

Finally, the influence of the melt pool temperature on the local mechanical properties was examined based on the hardness distribution over cross sections of individual weld beads. For this purpose, the samples produced with parameter set B at the highest as well as the lowest stable temperature [see Figs. 7(b) and 7(h)] were selected. Figure 9 shows the hardness maps of these samples, which were obtained based on 793 and 1213 individual hardness indentations, respectively. In both cases, the contour of the melt pool was superimposed with a dashed line corresponding to the fusion line in the cross section.

In the hardness maps, the solidified melt pool can be clearly identified from a drop in the hardness compared to the substrate

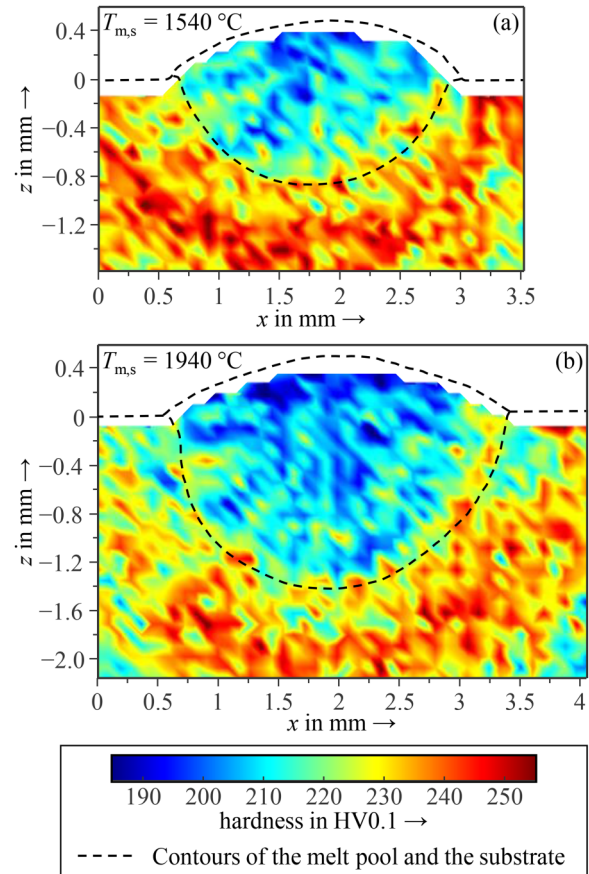


FIG. 9. Hardness maps of the samples produced with parameter set B at a melt pool temperature of (a) 1540 and (b) 1940 °C.

material. For both samples, the lowest hardness values (190–200 HV) were measured in the area close to the melt pool surface, where the highest temperatures occurred during the process. Toward the fusion line, a gradual increase in hardness could be observed. In the substrate material, hardness values between 215 HV and 255 HV were found. Moreover, a higher temperature resulted in an overall lower hardness of the solidified melt pool.

It is hypothesized that these observations are related to the occurring cooling rates as a result of the different energy inputs per unit length. The higher melt pool temperature is, thus, associated with a lower cooling rate, which leads to coarsening of the grain structure according to solidification theory.³³ To confirm this, a grain size analysis was performed according to ASTM E112, where five measurements were taken for each sample following the Abrams Three-Circle Procedure. This yielded an average ASTM grain size number G of 12.7 for a melt pool temperature of 1540 °C and 12.0 for 1940 °C. Thus, the average grain size was smaller at a lower melt pool temperature. Therefore, an increase in grain size is most likely the dominant mechanism for the decrease in hardness at a higher melt pool temperature.

11 March 2025 13:03:48

IV. CONCLUSIONS AND OUTLOOK

In this work, the cause-effect relationships between the melt pool temperature and the resulting weld bead characteristics were investigated in detail for laser metal deposition with coaxial wire feeding. This was enabled by using a dedicated closed-loop control system based on an in-axis pyrometer signal, where the laser power was used as the manipulated variable and was commanded by a proportional integral controller. First, a process window was determined for different parameter sets in which the temperature could be controlled in a stable manner without the occurrence of defects. Higher temperatures were associated with higher mean laser powers as well as increased melt pool dynamics, which manifested themselves in higher fluctuations in the temperature signal. Subsequently, the effects on the resulting weld bead characteristics were investigated in detail within this process window. A distinct positive correlation between the surface temperature of the melt pool and the weld bead width was demonstrated. Regarding the weld bead height, only for the parameter set with the lowest deposition rate, a clear correlation was evident. For the degree of dilution, a strong correlation with the melt pool temperature was found through the evaluation of cross sections, with higher temperatures and lower deposition rates leading to a higher volume of the melted substrate material. Furthermore, for a higher melt pool temperature, a lower hardness was determined within the solidified weld bead, which was attributed to a coarser grain structure resulting from its decreased cooling rate.

The findings obtained provide the foundation for further studies on temperature-controlled wire-based laser metal deposition as they will facilitate the selection of a suitable melt pool temperature and the interpretation of the melt pool temperature signal, respectively. In future work, the thermally controlled buildup of multilayer parts will be investigated. In this regard, for higher layers, it should be considered that low temperatures within the process window may not be attainable due to the altered conditions of heat conduction. In this respect, great attention has to be paid to suitable setpoint temperatures at different heights of the part to be produced. In this context, a layer-to-layer control similar to the approach of Tang and Landers²¹ with an adjustment of the laser power depending on the average temperature of the last layer could prove beneficial. This approach can contribute to process stability since fluctuations in the pyrometer signal due to varying melt pool shapes and, thus, changed radiation angles in higher layers can potentially be avoided. Moreover, it has to be considered that in a wire-based process the feedstock material has to be fully melted at all times in order to maintain a stable process. For this reason, appropriate limits on the specified laser power should be included in order to avoid the defect patterns of stubbing and dripping. Through a controlled heat input, it will be possible to avoid time-consuming parameter studies for novel part geometries. Furthermore, in order to obtain a fully controlled LMD process, a multivariable control will be implemented, through which the layer height as well as the heat input into the component are adjusted simultaneously.

ACKNOWLEDGMENTS

The results presented were achieved within the AdDEDValue project, which is supported by the German Federal Ministry for

Economic Affairs and Climate Action (BMWK) within the funding program “Digitalization of Vehicle Manufacturers and the Supplier Industry” (Contract No. 13IK002L) and supervised by the VDI Technology Center (VDI TZ). We would like to thank the BMWK and the VDI TZ for their support and for the effective and trusting cooperation. Furthermore, we would like to thank our partners Precitec GmbH & Co. KG, Sensortherm GmbH, and DINSE GmbH for providing the systems used.

AUTHOR DECLARATIONS

Conflict of Interest

The authors have no conflicts to disclose.

Author Contributions

Christian Bernauer: Conceptualization (lead); Data curation (lead); Formal analysis (lead); Funding acquisition (equal); Investigation (lead); Methodology (lead); Project administration (equal); Software (lead); Validation (lead); Visualization (lead); Writing – original draft (lead); Writing – review & editing (equal). **Avelino Zapata:** Methodology (supporting); Writing – review & editing (equal). **Michael Zaeh:** Funding acquisition (lead); Project administration (lead); Resources (lead); Supervision (lead); Writing – review & editing (equal).

REFERENCES

- ¹M. Schmidt, M. Merklein, D. Bourell, D. Dimitrov, T. Hausotte, K. Wegener, L. Overmeyer, F. Vollertsen, and G. N. Levy, “Laser based additive manufacturing in industry and academia,” *CIRP Ann.* **66**, 561–583 (2017).
- ²A. Dass and A. Moridi, “State of the art in directed energy deposition: From additive manufacturing to materials design,” *Coatings* **9**, 418 (2019).
- ³D. Ding, Z. Pan, D. Cuiuri, and H. Li, “Wire-feed additive manufacturing of metal components: Technologies, developments and future interests,” *J. Adv. Manuf. Technol.* **81**, 465–481 (2015).
- ⁴M. F. Steiner, M. Speier, J. Kelbassa, T. Schopphoven, and C. L. Häfner, “Influence of tool path planning on process stability and deposition accuracy in laser material deposition with coaxial wire feed,” *J. Laser Appl.* **34**, 12026 (2022).
- ⁵M. Bambach, I. Sizova, F. Kies, and C. Haase, “Directed energy deposition of Inconel 718 powder, cold and hot wire using a six-beam direct diode laser set-up,” *Addit. Manuf.* **47**, 102269 (2021).
- ⁶M. Heilemann, V. Jothi Prakash, L. Beulting, and C. Emmelmann, “Effect of heat accumulation on the single track formation during laser metal deposition and development of a framework for analyzing new process strategies,” *J. Laser Appl.* **33**, 012003 (2021).
- ⁷S. Donadello, V. Furlan, A. G. Demir, and B. Previtali, “Interplay between powder catchment efficiency and layer height in self-stabilized laser metal deposition,” *Opt. Lasers Eng.* **149**, 106817 (2022).
- ⁸H. Wang, W. Liu, Z. Tang, Y. Wang, X. Mei, K. M. Saleheen, Z. Wang, and H. Zhang, “Review on adaptive control of laser-directed energy deposition,” *Opt. Eng.* **59**, 070901 (2020).
- ⁹T. Hua, C. Jing, L. Xin, Z. Fengying, and H. Weidong, “Research on molten pool temperature in the process of laser rapid forming,” *J. Mater. Process. Technol.* **198**, 454–462 (2008).
- ¹⁰G. Bi, A. Gasser, K. Wissenbach, A. Drenker, and R. Poprawe, “Identification and qualification of temperature signal for monitoring and control in laser cladding,” *Opt. Lasers Eng.* **44**, 1348–1359 (2006).

- ¹¹G. Bi, A. Gasser, K. Wissenbach, A. Drenker, and R. Poprawe, "Investigation on the direct laser metallic powder deposition process via temperature measurement," *Appl. Surf. Sci.* **253**, 1411–1416 (2006).
- ¹²M. Pavlov, D. Novichenko, and M. Doubenskaia, "Optical diagnostics of deposition of metal matrix composites by laser cladding," *Phys. Procedia* **12**, 674–682 (2011).
- ¹³M. Doubenskaia, I. Smurov, S. Grigoriev, M. Pavlov, and E. Tikhonova, "Optical monitoring in elaboration of metal matrix composites by direct metal deposition," *Phys. Procedia* **39**, 767–775 (2012).
- ¹⁴M. Kotar, M. Fujishima, G. N. Levy, and E. Govekar, "Advances in the understanding of the annular laser beam wire cladding process," *J. Mater. Process. Technol.* **294**, 117105 (2021).
- ¹⁵T. E. Abioye, J. Folkes, and A. T. Clare, "A parametric study of Inconel 625 wire laser deposition," *J. Mater. Process. Technol.* **213**, 2145–2151 (2013).
- ¹⁶A. Zapata, C. Bernauer, C. Stadter, C. G. Kolb, and M. F. Zaeh, "Investigation on the cause-effect relationships between the process parameters and the resulting geometric properties for wire-based coaxial laser metal deposition," *Metals* **12**, 455 (2022).
- ¹⁷N. G. Mbodj, M. Abuabiah, P. Plapper, M. El Kandaoui, and S. Yaacoubi, "Bead geometry prediction in laser-wire additive manufacturing process using machine learning: Case of study," *Appl. Sci.* **11**, 11949 (2021).
- ¹⁸J. T. Hofman, B. Pathiraj, J. van Dijk, D. F. de Lange, and J. Meijer, "A camera based feedback control strategy for the laser cladding process," *J. Mater. Process. Technol.* **212**, 2455–2462 (2012).
- ¹⁹L. Song and J. Mazumder, "Feedback control of melt pool temperature during laser cladding process," *IEEE Trans. Control Syst. Technol.* **19**, 1349–1356 (2011).
- ²⁰L. Tang and R. G. Landers, "Melt pool temperature control for laser metal deposition processes—Part I: Online temperature control," *J. Manuf. Sci. Eng.* **132**, 011010 (2010).
- ²¹L. Tang and R. G. Landers, "Melt pool temperature control for laser metal deposition processes—Part II: Layer-to-layer temperature control," *J. Manuf. Sci. Eng.* **132**, 011011 (2010).
- ²²Z. Smoqi, B. D. Bevans, A. Gaikwad, J. Craig, A. Abul-Haj, B. Roeder, B. Macy, J. E. Shield, and P. Rao, "Closed-loop control of melt pool temperature in directed energy deposition," *Mater. Des.* **215**, 110508 (2022).
- ²³B. T. Gibson, Y. K. Bandari, B. S. Richardson, W. C. Henry, E. J. Vetland, T. W. Sundermann, and L. J. Love, "Melt pool size control through multiple closed-loop modalities in laser-wire directed energy deposition of Ti-6Al-4V," *Addit. Manuf.* **32**, 100993 (2020).
- ²⁴D. Salehi and M. Brandt, "Melt pool temperature control using LabVIEW in Nd:YAG laser blown powder cladding process," *Int. J. Adv. Manuf. Technol.* **29**, 273–278 (2006).
- ²⁵A. Zapata, C. Bernauer, M. Hell, H. Kriz, and M. F. Zaeh, "Direction-independent temperature monitoring for laser metal deposition with coaxial wire feeding," *Procedia CIRP* **111**, 302–307 (2022).
- ²⁶H. Fukuyama, H. Higashi, and H. Yamano, "Normal spectral emissivity, specific heat capacity, and thermal conductivity of type 316 austenitic stainless steel containing up to 10 mass% B4C in a liquid state," *J. Nucl. Mater.* **568**, 153865 (2022).
- ²⁷C. J. Bernauer, A. Zapata, L. Kick, T. Weiss, M. E. Sigl, and M. F. Zaeh, "Pyrometry-based closed-loop control of the melt pool temperature in laser metal deposition with coaxial wire feeding," *Procedia CIRP* **111**, 296–301 (2022).
- ²⁸M. Motta, A. G. Demir, and B. Previtali, "High-speed imaging and process characterization of coaxial laser metal wire deposition," *Addit. Manuf.* **22**, 497–507 (2018).
- ²⁹K. C. Mills, *Recommended Values of Thermophysical Properties for Selected Commercial Alloys* (Elsevier, New York, 2002), pp. 135–142.
- ³⁰M. Akbari and R. Kovacevic, "Closed loop control of melt pool width in robotized laser powder-directed energy deposition process," *Int. J. Adv. Manuf. Technol.* **104**, 2887–2898 (2019).
- ³¹B. Leffler and S. Malm, "Volume changes accompanying solidification of some austenitic stainless steels," *Met. Technol.* **4**, 81–90 (1977).
- ³²R. Blondeau, *Metallurgy and Mechanics of Welding* (John Wiley & Sons, New York, 2008).
- ³³M. H. Farshidianfar, F. Khodabakhshi, A. Khajepour, and A. P. Gerlich, "Closed-loop control of microstructure and mechanical properties in additive manufacturing by directed energy deposition," *Mater. Sci. Eng., A* **803**, 140483 (2021).